A&A 673, L7 (2023)
https://doi.org/10.1051/0004-6361/202346410

Astronomy & Astrophysics

LETTER TO THE EDITOR

N-enhancement in GN-z11: First evidence for supermassive stars nucleosynthesis in proto-globular clusters-like conditions at high redshift?

C. Charbonnel[1,2], D. Schaerer[1,2], N. Prantzos[3], L. Ramírez-Galeano[1], T. Fragos[1], A. Kuruvanthodi[1], R. Marques-Chaves[1], and M. Gieles[4,5]

[1] Department of Astronomy, University of Geneva, Chemin Pégasi 51, 1290 Versoix, Switzerland
e-mail: corinne.charbonnel@unige.ch
[2] IRAP, UMR 5277 CNRS and Université de Toulouse, 14 Av. E.Belin, 31400 Toulouse, France
[3] Institut d'Astrophysique de Paris, UMR 7095 CNRS, Sorbonne Université, 98bis Bd Arago, 75014 Paris, France
[4] ICREA, Pg. Lluís Companys 23, 08010 Barcelona, Spain
[5] Institut de Ciències del Cosmos (ICCUB), Universitat de Barcelona (IEEC-UB), Martí i Franquès 1, 08028 Barcelona, Spain

Received 14 March 2023 / Accepted 14 April 2023

ABSTRACT

Unusually high N/O abundance ratios were recently reported for a very compact, intensively star-forming object GN-z11 at $z = 10.6$ from JWST/NIRSpec observations. We present an empirical comparison with the C, N, and O abundance ratios in Galactic globular clusters (GCs) over a large metallicity range. We show that hot hydrogen-burning nucleosynthesis within supermassive stars (SMS) formed through runaway collisions can consistently explain the observed abundances ratio in GN-z11 and in GCs. This suggests that a proto-globular cluster hosting a SMS could be at the origin of the strong N-enrichment in GN-z11. Our model predicts the behavior of N/O, C/O, and Ne/O ratios as a function of metallicity, which can be tested if high-z objects similar to GN-z11 are detected with JWST in the future. Further studies and statistics will help differentiate the proto-GC scenario from the Wolf-Rayet scenario that we quantify with a population synthesis model, and shed more light on this peculiar object.

Key words. galaxies: high-redshift – galaxies: ISM – galaxies: abundances – galaxies: star clusters: general

1. Introduction

The detection of unusually bright nitrogen NIII] and NIV] ultraviolet (UV) emission lines in the JWST/NIRSpec spectrum of GN-z11 (Bunker et al. 2023) revealed exceptional nitrogen enrichment in this high-z galaxy. The N/O abundance ratio in the interstellar medium (ISM) of GN-z11 derived by Cameron et al. (2023, see also Senchyna et al. 2023) is more than four times solar ($\log(N/O) \gtrsim -0.25$). This is more than one order of magnitude higher than what is usually found in low-redshift galaxies and HII regions of a similar low metallicity ($12+\log(O/H) \lesssim 8.0$), and even slightly higher than in galaxies with super-solar metallicities (e.g., Berg et al. 2019; Vincenzo et al. 2016). The C/O ratio of GN-z11 is compatible with normal values but poorly constrained (Cameron et al. 2023). Reports of other peculiar objects showing indications for high N/O exist, at low and intermediate redshift (e.g., James et al. 2009; Telles et al. 2014; Villar-Martín et al. 2004).

The peculiar abundance ratios inferred in GN-z11 cannot be explained by classical stellar yields and standard galactic chemical evolution. However, they are commonly found in globular clusters (GCs) which are known to form in the early Universe (Gratton et al. 2019, for a review). It is now firmly established that in each of these old, massive, and compact clusters, a large fraction of the stars – the so-called second population (2P) – show different levels of N-enrichment correlated to O and C depletion and to Na and Al enrichment (with the most extreme 2P stars exhibiting $\log(N/O) \gtrsim +0.4$), while the so-called first population (1P) stars have the same chemical composition as field halo stars of a similar metallicity (with typical $\log(N/O) \lesssim -1$). From the nucleosynthesis point of view, there is considerable evidence that 2P GC stars formed out of a mixture between the original proto-GC gas and the yields of hot H burning through the CNO cycle and the NeNa and MgAl chains that were ejected by short-lived 1P stars (so-called polluters) in their host proto-cluster (Prantzos et al. 2017, and references therein). No signature of high He enrichment and of other nucleosynthesis processes such as triple-α, s-process, and explosive nucleosynthesis was found in the vast majority of the GCs, except in the most massive ones that might be the remnants of dwarf galaxy nuclei (Marino et al. 2021). The same chemical peculiarities were found in all the GCs of the Milky Way and of the Local Group where they have been looked for (Milone et al. 2017; Larsen et al. 2022), as well as in extragalactic massive star clusters of an intermediate age down to ~2 Gyr (Martocchia et al. 2018; Bastian et al. 2019), pointing to similar early enrichment histories. However, they were never observed in less massive open clusters, implying a minimum cluster mass ($\gtrsim$ a few 10^4 $M_\odot$, $M_V \lesssim -5$; Bragaglia et al. 2017) for their formation.

Several scenarios invoking different types of polluters were proposed to explain GC abundance anomalies (Bastian & Lardo 2018, for a review). The most recent observational clues point

toward the nucleosynthesis contribution of exceptional 1P polluters such as super-massive stars (SMSs) as proposed by Denissenkov & Hartwick (2014). There is no consensus how such a star forms, but an attractive scenario in the GC context is that it forms via stellar collisions. Gieles et al. (2018) show that proto-star clusters hosting a large number of proto-stars ($\gtrsim 10^6$) accreting gas at a high rate ($\gtrsim 10^5\ M_\odot\,\mathrm{Myr}^{-1}$) can undergo runaway collisions leading to the formation of SMSs with masses between $\sim 10^3$ and $\sim 10^5\ M_\odot$ in 1 to 2 Myr, before two-body relaxation stops the contraction of the system. Additionally, the SMSs can be continuously rejuvenated by stellar collisions and thus process H at the required temperature to explain all the nucleosynthesis patterns while keeping their He content low, in agreement with GC photometric constraints (Milone et al. 2018). While spewing processed material via their strong wind, they can thus act as a conveyor belt and process much more material through hot H burning than the maximum mass it reaches during the proto-GC contraction, solving the mass budget problem that plagues other models (Charbonnel 2017). Last but not least, this SMS formation channel could occur at any redshift in massive star clusters that are compact enough, and therefore also in the compact core of GN-z11, which has a high stellar density, as is subsequently discussed below.

In this Letter, we argue that the same scenario could potentially explain the high log(N/O) abundance ratios in GN-z11 (Sect. 2). We examine its compatibility with other properties of this high-z object, and we discuss the alternative WR option (Sect. 3). We conclude and make predictions for future observations of high-z galaxies (Sect. 4).

2. GN-z11: Abundance ratios potentially resulting from CNO processing in a SMS in proto-GC-like conditions

2.1. Comparison with GC data

To put our hypothesis in the GC observational context (see also Senchyna et al. 2023), we chose four Galactic GCs that cover a large range of metallicity and for which C, N, and O abundance measurements are simultaneously available, and we show in Fig. 1 the values of log(N/O) and log(C/O) as a function of log(O/H) in their individual stars and in Milky Way (MW) field halo stars. We compare to GN-z11 and other' galaxies data. On the one hand, each cluster contains 1P stars that present the same abundance ratios as Galactic field stars and as low-redshift galaxies at the same metallicity. The typical log(N/O) of these objects (~ -1 to -2 for $12+\log(\mathrm{O/H}) < 8$) is well explained by the production of primary N by fast-rotating massive stars of very low metallicity (Chiappini et al. 2006; Meynet et al. 2017). On the other hand, the log(N/O) values in the 2P stars of the four GCs reach or even exceed the level observed in GN-z11. Similarly high log(N/O) ratios are ubiquitous in GCs, with the maximum values being found in the most metal-poor and/or the most massive GCs (Mészáros et al. 2020). Interestingly, the population of N-rich stars that has been found in the MW inner halo (Schiavon et al. 2017) present other chemical peculiarities as GC 2P stars, and are likely escapers from the GC population (Gieles & Gnedin 2023). The same agreement holds for log(C/O), although we note that no high values are found in 47 Tuc. This comparison empirically supports the possibility that the bright N emission lines compared to faint O lines in GN-z11 may result from the contamination of the gas of a massive and compact – proto-GC-like – star cluster by CNO-processed material from the same polluters as those required to explain GC abundance patterns (see also Senchyna et al. 2023).

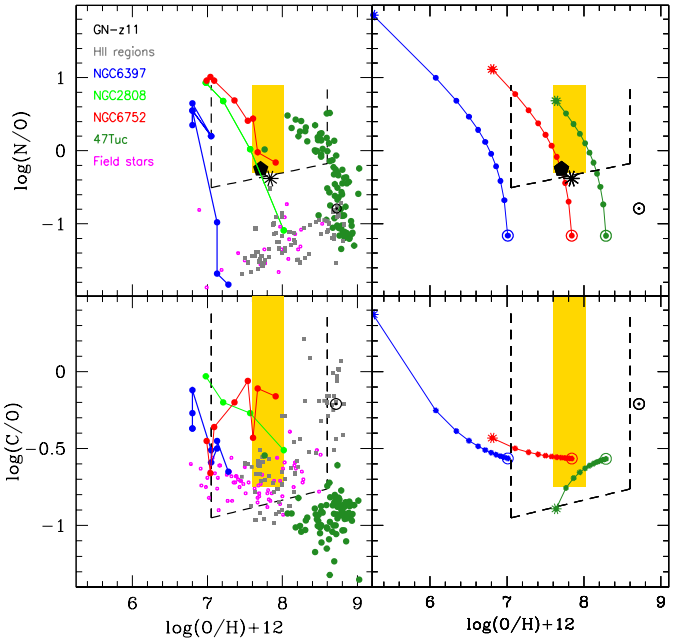

Fig. 1. Abundance ratios in GN-z11 and other environments, and a comparison with SMS models. The yellow box and the dashed black line show the location of the abundance ratios of GN-z11 from the Cameron et al. (2023) fiducial model and from their more conservative assumptions, respectively (with upper boundaries that are not well defined). The black pentagon and asterisk indicate the location of Senchyna et al. (2023) photoionization modeling results for GN-z11. Left: Abundance ratios in individual stars of four GCs (NGC 6397, Carretta et al. 2005; NGC 2808, Carlos et al. 2023; NGC 6752, Carretta et al. 2005; 47 Tuc, Mészáros et al. 2020), and in Milky Way field stars within the same metallicity range as the four GCs (Israelian et al. 2004; Akerman et al. 2004; Fabbian et al. 2009); for the GCs we have connected the points by line segments to guide the eye. The gray squares are the abundance ratios for extragalactic HII regions and galaxies (compilation from Izotov et al. 2023). Right: Theoretical abundance ratios as predicted from the dilution of the material of $10^4\ M_\odot$ SMS models with the assumed initial proto-GC abundances for the same metallicities as NGC 6397, NGC 6752, and 47 Tuc (blue, red, and green respectively). Along each GC sequence, the fraction of SMS H-processed material in the mixture decreases from one (pure SMS, asterisk symbols) to zero (pure proto-GC gas, open circles) with steps of 0.1 (full circles).

2.2. Comparison with SMS nucleosynthesis

Gieles et al. (2018) discuss how the maximum mass of a SMS formed via runaway collisions and the exact amount of H-processed material it ejects through winds depend on the uncertain stellar mass-radius relation and mass-loss rates adopted, as well as on the initial mass of the proto-GC where runaway collisions can occur. Using realistic assumptions based, for instance, on the properties of very massive stars and the results of collisional N-body simulations, they show that for the most massive proto-GC they consider and that hosts 10^7 proto-stars, the mass of the SMS can reach ~5% of the cluster stellar mass when the density of the cluster is maximum, and the mass it can process after 5 Myr is as high as $\sim 10^6\ M_\odot$ (corresponding to ~50% of the cluster stellar mass at that age).

To model nucleosynthesis in fastly growing SMSs, we computed evolution models for three metallicities ([Fe/H] = −0.72, −1.14, and –2 dex, assuming [α/Fe] = +0.3 dex) with the stellar evolution code MESA (Paxton et al. 2011, 2013, 2015, 2018, 2019; Jermyn et al. 2023). For a detailed description of our adopted stellar physics, we refer readers to Fragos et al. (2023, their Sect. 3). We started from a low-mass seed (0.7 $M_\odot$) and applied high-mass accretion rates to reach 10^4 $M_\odot$ in ∼0.15 Myr after the runaway collision process started, as predicted in the case of a proto-star cluster hosting 10^7 stars (for details, see Gieles et al. 2018). For this, we multiplied the prescription by Haemmerlé et al. (2019) for the accretion rate onto the star by a factor of ten. In these conditions, fresh H refills the star permanently and the central He-mass fraction stays close to its original value while the CNO cycle runs at equilibrium. The central temperature of the model thus increases very slowly while the stellar mass grows (for the lowest metallicity considered, T_c increases from 67 to 73 MK while the stellar mass increases from 3×10^3 to 10^4 $M_\odot$). Hence, we find that accreting SMSs satisfy the nucleosynthesis constraints over a large range of masses. We did not include mass loss, but we assume that once mass accretion and mass loss roughly compensate for each other, the conveyor belt for hot H burning is fully efficient as predicted by Gieles et al. (2018). Hence, the chemical properties of the SMS ejecta shall correspond to that of a "conveyor SMS" of the same mass. Depending on the initial number of proto-stars in the proto-GCs, the mass of the "conveyor SMS" and the amount of ejecta shall slightly vary, but their chemical properties remain similar.

In Fig. 1, we show the predictions for the log(N/O) and log(C/O) abundance ratios as a function of log(O/H)+12 in the convective interior of the models when the stellar mass has reached 10^4 $M_\odot$. The behavior of N/O versus O/H differs from that of C/O when the SMS metallicity changes. While the N enrichment results from the depletion of both C and O in the CNO cycle and occurs at all metallicity, C is relatively more depleted than O in higher metallicity SMSs (for a given SMS mass, the central temperature is lower at higher metallicity). As a consequence, while the N/O ratio always increases in the SMSs, with more extreme values due to stronger O depletion at lower metallicity, the C/O increases with respect to its initial value only in the most metal-poor case.

For each metallicity, we show in Fig. 1 a sequence of points that correspond to the abundance ratios predicted when the SMS material is mixed with the proto-GC gas in different proportions (Prantzos & Charbonnel 2006; Denissenkov & Hartwick 2014). The abundance ratios in GN-z11 require SMS ejecta being mixed with original proto-GC gas in proportions (the region where the models overlap with the boxes corresponding to GN-z11) that depend on the actual metallicity of GN-z11. This is in very good agreement with the dilution requirement to explain the abundance ratios in GCs, with well-known variations from one GC to another (as seen among the three GCs in Fig. 1), with the most extreme abundance ratios and the larger fraction of 2P versus 1P stars increasing with the GC mass and/or with decreasing metallicity (Milone et al. 2017; Masseron et al. 2019). This supports the super-linear correlation between the amount of mass that can be processed by a SMS and the mass of the cluster, as predicted by Gieles et al. (2018).

As a final comment on nucleosynthesis, we recall that 2P stars in GCs also show high Na and Al enrichment. If our claim that the peculiar N, C, and O abundance ratios in GN-z11 result from the same scenario as those in GCs, then its gas shall also be Na and Al enriched. Last but not least, it is mostly ^{22}Ne that is involved in the NeNa chain that leads to Na enrichment, while the more abundant ^{20}Ne is hardly changed in the SMS models. However, since O is strongly depleted, we predict that the Ne/O abundance ratio shall be higher in GN-z11 and other similar high-z objects that shall be found in the future compare to the case of normal galaxies of similar metallicities, with the highest Ne/O in the most metal-poor N-enriched objects.

3. Discussion

As just shown, the observed nebular abundances of GN-z11 are compatible with those of GCs and possibly due to CNO processing in SMSs formed via stellar collisions in massive and compact – proto-GC-like – star clusters. We now examine if other properties of this source are also compatible with this scenario and we discuss possible alternatives.

3.1. GN-z11: An extreme regime of a massive star cluster polluted by SMSs?

The size measurement and stellar mass estimate of Tacchella et al. (2023) translate to a compactness index $C_5 \gtrsim (M_\star/10^5\,M_\odot)\,(r_{\rm h}/{\rm pc})^{-1} \sim 200$, which is higher than that of old Galactic GCs and young extragalactic massive star clusters by a factor of ∼30 to 15 respectively, as the comparison with Krause et al. (2016) shows. The same holds for the mass surface density ($\sim 4 \times 10^4$ $M_\odot$ pc^{-2}) which is approximately one order of magnitude higher than that of a typical old GC, but compatible with that derived for the high-z densest clouds identified in high-z galaxies (Claeyssens et al. 2023). The stellar mass density (expressing the half mass within the half-light radius) $\rho_\star \gtrsim 600\,M_\odot$ pc^{-3} is also high but not extreme compared to YMCs and GCs (Baumgardt & Hilker 2018), and it remains a lower limit since the object is mostly unresolved. It is close to the initial stellar mass density considered by Gieles et al. (2018) for their GC formation scenario involving SMSs.

Next we examine if sufficient amounts of enriched gas are available to explain the observed abundance ratios. The total mass of enriched, ionized gas, which is directly observable, can easily be estimated assuming ionization equilibrium and a constant ISM density (see, e.g., Dopita & Sutherland 2003):

$$M_{\rm ionized} = \frac{m_{\rm p} Q_{\rm H}}{\alpha_B n_{\rm e}} = 2.2 \times 10^7 \left(\frac{10^3}{n_{\rm e}}\right)\left(\frac{Q_{\rm H}}{8.8 \times 10^{54}}\right) M_\odot, \quad (1)$$

where $Q_{\rm H}$ is the ionizing photon production rate that can be determined from H recombination lines, $n_{\rm e}$ the electron density, $m_{\rm p}$ the proton mass, and $\alpha_{\rm B}$ the recombination rate coefficient. The main unknown here is the $n_{\rm e}$, which cannot be determined using standard optical diagnostics (e.g. using [O II] λ3726,3729 doublet) from the available JWST observations of GN-z11, but which can be estimated from density-sensitive UV lines (Senchyna et al. 2023). The extreme compactness of GN-z11 clearly indicates higher-than-average densities. For example, the observed increase in $n_{\rm e}$ with SFR surface density at $z \sim 1$–3 (Reddy et al. 2023) suggests a minimum of $n_{\rm e} \gg 500$ cm^{-3}. Very high densities are possible and possibly expected (Dekel et al. 2023), but $n_{\rm e} \gg 10^5$ cm^{-3} is probably excluded since the [O II] λ3726,3729 emission doublet (which has the lowest critical density of the lines observed) would then be significantly weakened (Bunker et al. 2023). On the other hand, if the density is not uniform even higher electron densities could be reached in the core, as suggested by Senchyna et al. (2023).

Adopting the ionization rate derived from observations ($Q_{\rm H} = 8.8 \times 10^{54}$ s^{-1}, Bunker et al. 2023) and $n_{\rm e} = 10^5$ cm^{-3},

a plausible minimum mass of ionized gas is therefore $M_{\rm ionized} \sim 2 \times 10^5\,M_\odot$. Assuming that the gas has a constant density and uniform abundances, this implies that the amount of enriched material should be of the same order of $\gtrsim 10^5\,M_\odot$, assuming a dilution factor of 0.5. The scenario of Gieles et al. (2018) predicts enriched ejecta (wind) masses between $\sim 10^4$–$10^6\,M_\odot$, which are ejected over ~3 Myr from the SMS. From the currently available data, we therefore conclude that these amounts could be sufficient to significantly enrich the amount of ionized gas observed in GN-z11.

We can then ask if the core of GN-z11 is a single proto-GC-like object. Both the inferred stellar mass ($M_{\star\,\rm GN-z11} \sim 10^9\,M_\odot$) and the brightness of GN-z11 (~26 AB magnitudes in the rest-UV) are fairly high, but not unseen compared to observed values for stellar clumps observed at high redshift (see Claeyssens et al. 2023). However, the exact nature of these clumps is not known, and we cannot assert whether these entities and the unresolved core of GN-z11 represent individual clusters (e.g. scaled-up versions of 30 Doradus) or more complex regions. Clearly, for classical assumptions, GN-z11 is most likely too bright to host a single proto-GC-like cluster in the regime explored by Gieles et al. (2018). Assuming the UV emission of GN-z11 is dominated by a single young cluster with an age of ~5 Myr, the stellar mass would be $\sim 1.2 \times 10^8\,M_\odot$, using the model of Boylan-Kolchin (2017).

Now, the Initial Mass Function (IMF) could favor more massive stars at high z, for instance due to the rising Cosmic Microwave Background temperature, collisions in very dense media, or others (e.g., Steinhardt et al. 2022), in which case the inferred stellar mass would be lower. The presence of an SMS could potentially lower the stellar mass estimate even further. However, only for a maximum SMS mass of $M_{\rm SMS} \sim 10^6\,M_\odot$ explored by the scenario of Gieles et al. (2018), would the SMS reach a magnitude of $m_{\rm AB} \sim 27.5$ at $z \sim 10$, and the cluster plus SMS would then possibly reach $m_{\rm AB} \sim 27$, according to the predictions of Martins et al. (2020). It therefore seems difficult to explain the entire core of GN-z11 by a single SMS-hosting cluster, and we thus suggest that it contains other lower-mass star clusters, possibly hosting multiple very massive stars and/or SMSs. Last, it could eventually fall in the regime of the most massive GCs such as Ω Cen, M54, or NGC 1851, which present similar abundance patterns to GCs, while being the remnants of dwarf galaxy nuclei.

In any case, these simple estimates leave some room for the simple toy-model of Gieles et al. (2018) scenario to explain the currently available observations of GN-z11. However, we cannot definitively conclude on the "proto-GC" nature of this object.

3.2. Alternative scenarios, and the possible role of rotating massive star winds

Different scenarios to explain the peculiar abundance pattern of GN-z11 have been discussed by Cameron et al. (2023), albeit without quantitative estimates or models. These include the presence of a massive black hole, pollution from traditional evolved stars, the impact of primordial or exotic stellar evolution channels, tidal disruption events, or effects of stellar encounters in dense star clusters. None of these scenarios provide clear predictions, but for reasons discussed by Cameron et al. (2023), they favor tidal disruption events or runaway stellar collisions in a dense stellar cluster. Senchyna et al. (2023), on the other hand, noting the similarity between the N/O abundances in GC stars and GN-z11, have proposed that this object could show possible signatures of GC precursors, similarly to our claim.

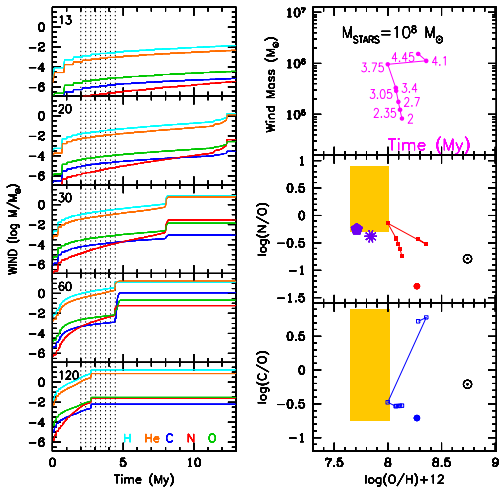

Fig. 2. Predictions for pollution from the winds of rotating massive stars. Left: Cumulative mass in the winds of selected massive stars of Limongi & Chieffi (2018) with a metallicity [Fe/H] = −1 and an initial rotational velocity of 300 km s^{-1} (mass in $M_\odot$ in the top left) as a function of time. Top right: Total mass ejected in the stellar winds of a starburst with a total mass of $10^8\,M_\odot$ with a Salpeter IMF at various times after the burst (as indicated in the left panels by dotted vertical lines) versus the O/H. Middle right: Corresponding evolution of the N/O when the ejecta are diluted in ambient gas of the same mass; observational data are the same as in Fig. 1. Bottom right: Same as in the middle panel, but for C/O.

Local enrichment from massive star winds, presumably in the Wolf-Rayet (WR) phase, have also been discussed in both the of above studies. To quantify this scenario, we have computed a population synthesis model using stellar wind yields of rotating massive stars with a metallicity of [Fe/H] = −1 and an initial rotational velocity of 300 km s^{-1} from Limongi & Chieffi (2018). Such yields have already been used in Prantzos et al. (2018) to successfully describe the chemical evolution of the solar neighborhood. The composition of the wind yields is shown in the left panels of Fig. 2. Assuming that stars more massive than 20–25 $M_\odot$ do not explode but collapse and become black holes (see Prantzos et al. 2018), the ejecta have exclusively a wind composition for several million years; they are dominated early on by H-burning products (N-rich and O- and C-poor during the WN phase) and later by He-burning products (N-poor and C- and O- rich during the WC phase). Assuming a starburst of $10^8\,M_\odot$ formed within 1 Myr with a Salpeter IMF, the mass ejected after the first few million years is of the order of $10^6\,M_\odot$ (Fig. 2, top right panel), which is comparable to the gas mass estimates discussed above. For a short period, lasting a few 10^5 yr (as seen from the time line in the top right panel), the N/O and C/O values of the ejecta – assumed to have been diluted to equal mass of the original gas – reach the range of values reported for GN-z11; this period ends after ~3.7 Myr (similar to the age reported in Senchyna et al. 2023), when He-burning products lead to strong C and O enrichment of the stellar winds.

The above scenario is fairly simplistic (ignoring, among many other things, the role of binarity in the formation of WR stars) and is presented for illustration purposes. In contrast to the SMS scenario, it is not related to GCs, since their defining feature (the Na-O anticorrelation) cannot be produced by "normal" massive stars (Prantzos et al. 2017). Additionally, it requires a rather special timing since the WN period "favorable" to enhance N/O is, at best, ~1/10 of the duration of the starburst, which is

estimated to only a few million years in GN-z11 (Cameron et al. 2023; Senchyna et al. 2023).

Local enrichment of N/O (and C/O in a few cases) reaching the levels shown in Fig. 2, has been observed in some HII regions hosting WR stars (e.g., López-Sánchez et al. 2007). In general, however, and measured on larger scales, the N enrichment observed in WR galaxies is very modest, with average N/O enhancements of the order of ∼0.1 dex only (Brinchmann et al. 2008). Furthermore, signatures of WR stars are not detected in GN-z11, or extremely weak at best, as pointed out by Bunker et al. (2023), Cameron et al. (2023), and Senchyna et al. (2023). Finally, except for one peculiar galaxy showing WR features, Mrk 996, none have so far shown the strong UV emission lines of N III] λ1750 or N IV] λ1486 observed in GN-z11 (cf. Senchyna et al. 2023). The hypothesis of pollution from WR stars is therefore debatable.

In addition to the points discussed previously, other indirect arguments favoring the explanation of SMSs caught in the act of polluting proto-GC-like massive star clusters might also be mentioned. For example, it is known to require extremely compact and dense environments, as those found in GN-z11; the oldest MW GCs have absolute ages of ∼13.6 ± 1.6 Gyr (O'Malley et al. 2017), making it possible to have GC-like forming conditions at very high z, even though the peak of GC formation is predicted to be at z around four in current hierarchical assembly models (e.g., El-Badry et al. 2019). The interpretation of GN-z11 as a GC progenitor may imply that these models and the role of GCs in reionization need to be reconsidered. On the other hand, WR stars form in all conditions and at all times (of course with variable amounts depending on metallicity and other factors). Therefore, abundance patterns resembling those of GC stars should be found more frequently in ionized gas at high z and related to very compact sources. For a single object, such "statistical" arguments are, however, not properly applicable. Future observations and other studies should allow for these and alternative scenarios to be further refined and tested.

4. Conclusions

In this Letter, we present an empirical comparison of the C, N, and O abundance ratios in the compact $z = 10.6$ galaxy GN-z11 derived recently from JWST observations with data in GC and field star observations, and a quantitative estimate of SMS nucleosynthesis that can form through runaway collisions in proto-GCs, as proposed in the scenario of Gieles et al. (2018). We show that the SMS polluter models can simultaneously explain the observations of GN-z11 and of the GCs, with similar dilution values between the H-processed material in the SMS and the original proto-GC gas. Our model predicts that similarly high or even higher N/O and C/O ratios could be observed in proto-GCs in high-z galaxies with a lower metallicity than GN-z11, but that lower C/O ratios shall be expected for higher metallicities. On the other hand, the Ne/O ratios in similar objects shall be higher than in normal galaxies of similar metallicities, with an increase inversely proportional to the metallicity of the proto-GC host galaxy. Finally, N-enriched and O-depleted gas in GN-z11 should also be enriched in Na and Al and in similar high-z objects, if the observations reflect the conditions during GC formation. Alternatively, the "rotating massive star winds" scenario could also explain the peculiar abundance patterns observed in GN-z11, but within a rather short time window, at least with current stellar models. In view of the scarce current observational sample, this option cannot be totally excluded at present. However, in this case GN-z11 cannot be host of a proto-GC, as massive stars will later pollute their environment in He-burning products, which is at odds with observed abundances in GCs today.

If the SMS scenario can be firmed up by future studies, this would provide an important step for our understanding of GCs and for the formation of SMSs in general, with numerous important implications. In any case, the peculiar properties of GN-z11 just revealed by JWST call for further studies to understand the physical processes ongoing in such extreme objects in the early Universe, and their possible connection with the formation of globulars, SMSs, potentially also supermassive black holes among others (see discussions in Cameron et al. 2023; Senchyna et al. 2023).

Acknowledgements. We thank the anonymous referee for constructive comments and Y. Izotov for providing data. CC acknowledges support from the Swiss National Science Foundation (SNF; Project 200020-192039). LRG and TF acknowledge support from a SNF Professorship grant (Project No PP00P2_211006). MG acknowledges support from the Ministry of Science and Innovation (EUR2020-112157, PID2021-125485NB-C22) and from Grant CEX2019-000918-M funded by MCIN/AEI/10.13039/501100011033 and from AGAUR (SGR-2021-01069).

References

Akerman, C. J., Carigi, L., Nissen, P. E., Pettini, M., & Asplund, M. 2004, A&A, 414, 931
Bastian, N., & Lardo, C. 2018, ARAA, 56, 83
Bastian, N., Usher, C., Kamann, S., et al. 2019, MNRAS, 489, L80
Baumgardt, H., & Hilker, M. 2018, MNRAS, 478, 1520
Berg, D. A., Erb, D. K., Henry, R. B. C., Skillman, E. D., & McQuinn, K. B. W. 2019, ApJ, 874, 93
Boylan-Kolchin, M. 2017, MNRAS, 472, 3120
Bragaglia, A., Carretta, E., D'Orazi, V., et al. 2017, A&A, 607, A44
Brinchmann, J., Kunth, D., & Durret, F. 2008, A&A, 485, 657
Bunker, A. J., Saxena, A., Cameron, A. J., et al. 2023, A&A, submitted [arXiv:2302.07256]
Cameron, A. J., Katz, H., Rey, M. P., & Saxena, A. 2023, MNRAS, submitted [arXiv:2302.10142]
Carlos, M., Marino, A. F., Milone, A. P., et al. 2023, MNRAS, 519, 1695
Carretta, E., Gratton, R. G., Lucatello, S., Bragaglia, A., & Bonifacio, P. 2005, A&A, 433, 597
Charbonnel, C. 2017, in Formation, Evolution, and Survival of Massive Star Clusters, eds. C. Charbonnel, & A. Nota, 316, 1
Chiappini, C., Hirschi, R., Meynet, G., et al. 2006, A&A, 449, L27
Claeyssens, A., Adamo, A., Richard, J., et al. 2023, MNRAS, 520, 2180
Dekel, A., Sarkar, K. S., Birnboim, Y., Mandelker, N., & Li, Z. 2023, ArXiv eprints [arXiv:2303.04827]
Denissenkov, P. A., & Hartwick, F. D. A. 2014, MNRAS, 437, L21
Dopita, M. A., & Sutherland, R. S. 2003, Astrophysics of the Diffuse Universe (Berlin, New York: Springer)
El-Badry, K., Quataert, E., Weisz, D. R., Choksi, N., & Boylan-Kolchin, M. 2019, MNRAS, 482, 4528
Fabbian, D., Nissen, P. E., Asplund, M., Pettini, M., & Akerman, C. 2009, A&A, 500, 1143
Fragos, T., Andrews, J. J., Bavera, S. S., et al. 2023, ApJS, 264, 45
Gieles, M., & Gnedin, O. 2023, MNRAS, submitted [arXiv:2303.03791]
Gieles, M., Charbonnel, C., Krause, M. G. H., et al. 2018, MNRAS, 478, 2461
Gratton, R., Bragaglia, A., Carretta, E., et al. 2019, A&A Rv., 27, 8
Haemmerlé, L., Eggenberger, P., Ekström, S., et al. 2019, A&A, 624, A137
Israelian, G., Ecuvillon, A., Rebolo, R., et al. 2004, A&A, 421, 649
Izotov, Y. I., Schaerer, D., Worseck, G., et al. 2023, MNRAS, 522, 1228
James, B. L., Tsamis, Y. G., Barlow, M. J., et al. 2009, MNRAS, 398, 2
Jermyn, A. S., Bauer, E. B., Schwab, J., et al. 2023, ApJS, 265, 15
Krause, M. G. H., Charbonnel, C., Bastian, N., & Diehl, R. 2016, A&A, 587, A53
Larsen, S. S., Eitner, P., Magg, E., et al. 2022, A&A, 660, A88
Limongi, M., & Chieffi, A. 2018, ApJS, 237, 13
López-Sánchez, Á. R., Esteban, C., García-Rojas, J., Peimbert, M., & Rodríguez, M. 2007, ApJ, 656, 168
Marino, A. F., Milone, A. P., Renzini, A., et al. 2021, ApJ, 923, 22
Martins, F., Schaerer, D., Haemmerlé, L., & Charbonnel, C. 2020, A&A, 633, A9
Martocchia, S., Cabrera-Ziri, I., Lardo, C., et al. 2018, MNRAS, 473, 2688
Masseron, T., García-Hernández, D. A., Mészáros, S., et al. 2019, A&A, 622, A191

Mészáros, S., Masseron, T., García-Hernández, D. A., et al. 2020, MNRAS, 492, 1641
Meynet, G., Maeder, A., Choplin, A., et al. 2017, in 14th International Symposium on Nuclei in the Cosmos (NIC2016), eds. S. Kubono, T. Kajino, S. Nishimura, et al., 010401
Milone, A. P., Piotto, G., Renzini, A., et al. 2017, MNRAS, 464, 3636
Milone, A. P., Marino, A. F., Renzini, A., et al. 2018, MNRAS, 481, 5098
O'Malley, E. M., Gilligan, C., & Chaboyer, B. 2017, ApJ, 838, 162
Paxton, B., Bildsten, L., Dotter, A., et al. 2011, ApJS, 192, 3
Paxton, B., Cantiello, M., Arras, P., et al. 2013, ApJS, 208, 4
Paxton, B., Marchant, P., Schwab, J., et al. 2015, ApJS, 220, 15
Paxton, B., Schwab, J., Bauer, E. B., et al. 2018, ApJS, 234, 34
Paxton, B., Smolec, R., Schwab, J., et al. 2019, ApJS, 243, 10
Prantzos, N., & Charbonnel, C. 2006, A&A, 458, 135
Prantzos, N., Charbonnel, C., & Iliadis, C. 2017, A&A, 608, A28
Prantzos, N., Abia, C., Limongi, M., Chieffi, A., & Cristallo, S. 2018, MNRAS, 476, 3432
Reddy, N. A., Sanders, R. L., Shapley, A. E., et al. 2023, ApJ, submitted [arXiv:2302.10213]
Schiavon, R. P., Zamora, O., Carrera, R., et al. 2017, MNRAS, 465, 501
Senchyna, P., Plat, A., Stark, D. P., & Rudie, G. C. 2023, AAS J., submitted [arXiv:2303.04179]
Steinhardt, C. L., Sneppen, A., Mostafa, B., et al. 2022, ApJ, 931, 58
Tacchella, S., Eisenstein, D. J., Hainline, K., et al. 2023, ApJ, submitted [arXiv:2302.07234]
Telles, E., Thuan, T. X., Izotov, Y. I., & Carrasco, E. R. 2014, A&A, 561, A64
Villar-Martín, M., Cerviño, M., & González Delgado, R. M. 2004, MNRAS, 355, 1132
Vincenzo, F., Belfiore, F., Maiolino, R., Matteucci, F., & Ventura, P. 2016, MNRAS, 458, 3466